Biophysical Journal, Volume *110*

Supplemental Information

Actomyosin Cortical Mechanical Properties in Nonadherent Cells Determined by Atomic Force Microscopy

Alexander X. Cartagena-Rivera, Jeremy S. Logue, Clare M. Waterman, and Richard S. Chadwick

Supporting Information Text, Figures, and Table

Supporting Information Text S1

Theory for surface tension, hydrostatic pressure, and elasticity using the AFM

1. Calculation of surface tension and hydrostatic pressure.

Consider a tipless AFM microcantilever with known spring constant k_c (N/m) is being approached and pushed against a spherical or hemispherical object with initial radius R (m). The sample whose mechanical properties are characterized by surface tension T (N/m), elastic Young's Modulus E (Pa), and hydrostatic pressure P (Pa), is compressed and undergoes small deformation compared to its original radius <10%R. In order to derive analytical expressions to solve for the object surface tension, elastic modulus, and hydrostatic pressure; some assumptions are needed to be satisfied:

1. Induced deformation is small compared to initial radius (less than 10%R). Contact area is small compared to initial radius.
2. Viscoelastic contribution can be neglected.
3. Cytoplasmic elasticity and cortex bending are negligible.
4. In low-strain regime the mechanical and geometrical properties behave mostly linear, by contrast, high-strains the properties behaves highly nonlinear [1].
5. Weak adhesions and small deviation for sphericity have a negligible effect.
6. Volume, internal pressure, and tension are constant during AFM ramp.

For the sake of simplicity, we are treating the system as a spherical sample being slightly deformed by a flat and smooth surface. Applying conservation of volume and pressure, it follows that:

Constant Volume:
$$\frac{4}{3}\pi R^3 = \frac{4}{3}\pi a^2 b\ ,$$
$$a = \sqrt{R^3/_b}\ , \tag{S1}$$

Law of Laplace:
$$P\pi R^2 = 2\pi RT\ ,$$
$$P = \frac{2T}{R}\ , \tag{S2}$$

where R is the initial radius (m), a is the horizontal deformed shape radius (m), b is the vertical deformed shape radius (m), P is the hydrostatic pressure (Pa), and T is the surface tension (N/m). When the cantilever is pressed on the sample it causes a deformation Δ (m) that is given by the relationship of the geometric parameters R and b; $\Delta = R - b$. Now, performing a force balance with compressive cantilever force F (N):

$$P\pi a^2 = 2\pi aT + F\ . \tag{S3}$$

Substituting Equations S1 and S2 into Equation S3 and rearranging terms yield:

$$2\pi T\left[\frac{R^2}{R-\Delta}-\sqrt{\frac{R^3}{R-\Delta}}\right]=F\,. \tag{S4}$$

In the small strain regime, we apply Taylor series expansion to **Eq. S4**:

$$2\pi T\left\{R\left(1+\frac{\Delta}{R}+\cdots\right)-R\left(1+\frac{1}{2}\frac{\Delta}{R}+\cdots\right)\right\}=F\,. \tag{S5}$$

In Equation S5, compressive cantilever force *F* applied to the sample is given by $F=k_c d$, where k_c is the calibrated cantilever spring constant (N/m), and *d* is the cantilever deflection (m). Substituting *F* into Equation S5 and simplifying for only 1st order term and discarding higher order term contribution we get:

$$\pi T\Delta = k_c d\,. \tag{S6}$$

The sample deformation is given by the relationship $d=Z-Z_0-\Delta$, where Z_0 is the contact point (m). Lastly, substituting d relationship into Equation S6 and solving for *T*:

$$T=\frac{k_c}{\pi}\left(\frac{1}{Z/_d-1}\right). \tag{S7}$$

This equation Equation S7 directly solve for surface tension by fitting the initial linear portion of a force-distance curve. Afterwards, the hydrostatic pressure can be obtained by using Equation S2. We use Equations S2 and S7 in the main article to estimate the surface tension and hydrostatic pressure of water-in-oil microdrops and nonadherent fibroblast cells.

2. Calculation of elastic moduli.

With the aforementioned approach we can calculate the surface tension of the round sample and this value can be used to calculate the elasticity Young's modulus *E* (Pa) of the actomyosin cortex of nonadherent fibroblasts. To do that, the sample tensile stress is given by the expression:

$$\sigma=\frac{T}{h}, \tag{S8}$$

where *h* is the cortex thickness (m). Hooke's law relates the Young's modulus of a material to the stress and strain:

$$E=\frac{\sigma}{\epsilon}, \tag{S9}$$

where ϵ is the localized cortex strain $\epsilon=\frac{R'-R}{R}=\frac{R'}{R}-1$. Here $R'=\frac{a^2}{b}$ is the local flattened radius of curvature of an ellipsoid, where *a* is the major dimension and *b* is the minor dimension of the flattened

ellipsoid. Because a small deformation is applied to the spherical specimen $R' = \frac{a^2}{b} = \frac{R^3}{b^2}$. When the cantilever is pressed on the object it causes a small deformation *Δ* that is given by the relationship of the geometric parameters *R* and *b*; $\Delta = R - b$, as previously presented. Now, solving for the local strain we get

$$\epsilon = \left(\frac{\Delta}{b}\right)^2 + 2\frac{\Delta}{b} + 1 - 1 \approx 2\frac{\Delta}{b}, \tag{S10}$$

$\epsilon \approx 2\frac{\Delta}{b}$ because *b* is much larger than the small indentation Δ. Substituting Equations S8 and S10 into Equation S9 the final result for the elastic Young's modulus is:

$$E = \frac{\pi R T^2}{2hk_c d}. \tag{S11}$$

Supporting Information Text S2

The bending contribution can be neglected in nonadherent cells

The contribution of bending forces of the actin cortex has been shown to be important for in the lamellipod of adherent cells [2]. However, for nonadherent cells this is not well understood yet. The forces generated by the contractile actomyosin cortex are identified as bending and tensile forces. The nonadherent cell is assumed to be of spherical shape and is deformed by a tipless AFM cantilever. We assume that both tension and bending forces resist the cantilever-induced deformation. Thus, using the dimensionless equation of a shell relating bending and tension forces given in [3] and modified for spherical shape:

$$\frac{Bending\ forces}{Tensile\ forces} \sim \frac{D}{TR^2}, \tag{S12}$$

where D (N-m) is the bending modulus, T (N/m) is the actin cortex tension, and R (m) is the cell initial radius. Now, introducing the relation of bending modulus to elastic modulus and solving, we get:

$$\frac{Bending\ forces}{Tensile\ forces} \sim \frac{1}{9}\left(\frac{Eh}{T}\right)\left(\frac{h}{R}\right)^2, \tag{S13}$$

where E (Pa) is the cortex elastic modulus and h (m) is the cortex thickness. This relation allows the comparison of bending and tensile forces using the measured parameters obtained by our method. Table S1 shows the data collected from live nonadherent HFF cells with and without pharmacological drug treatments. The values of the calculated ratio are substantially small 0.01-0.05%, meaning that the contribution of bending forces in nonadherent cells is basically negligible.

Supporting Information Text S4

Contact radius between AFM cantilever and nonadherent cell is insignificant for small deformations

By pressing the flat cantilever on a nonadherent rounded cell it can potentially create a large contact area between the AFM cantilever and the cell, suggesting that we could have interfacial tension contribution. We have made a calculation to estimate the contact radius between the flat cantilever and the round cell. We can also show that the contact radius is very small for 30 nm deflection of the cantilever. For Hertz contact mechanics theory the contact radius *a* is given by

$$\frac{a}{R} = \sqrt[3]{\frac{9k_c d}{16E_{cortex}R^2}}. \qquad \text{(S14)}$$

Taking k_c= 0.09 N/m, *d*= 30 nm, E_{cortex}= 42 kPa, and *R*= 8 μm gives a a/R=0.083. This overestimates the contact radius since it implies a flattening of the sphere by an amount $\delta = 1/2\,(a/R)^2 R$= 27.4 nm. Taking into account that the cantilever is bent upwards by 30 nm gives an actual flattening of δ'=2.6 nm. From $\delta' = 1/2\left(a'/R\right)^2 R$, we obtain a'=204 nm as the actual contact radius. This result implies that the contact radius is less than 3% the cell radius.

Supporting Information Text S3

Cytoplasmic viscoelastic and purely elastic contributions are negligible in nonadherent cells

By velocity-dependent compression force curves performed on the same nonadherent HFF cell (Figure 3D and Fig. S3), we showed that viscoelastic contributions are negligible for small deformations less than or equal to ≤400 nm. However, cytoplasm elastic response may potentially contribute. We perform calculations that show that cytoplasmic elastic response is ≤7% of the cortical elastic response. To justify the assumption that there is a negligible elastic response from the cytoplasm we can show that the elastic energy to deform the cytoplasm is a small fraction of the elastic energy to deform the cortex. Consider first the cytoplasm. The elastic energy per unit volume (N-m/m^3 is ${}^1\!/_2\, E_{cyto}\left(\varepsilon_{xx}^2+\varepsilon_{yy}^2+\varepsilon_{zz}^2\right)$ where the strains can be related to the deformation Δ of the sphere: $\varepsilon_{zz}={}^{\Delta}\!/_{(2R)}$; and $\varepsilon_{xx}=\varepsilon_{yy}=\left({}^{R}\!/_{(R-\Delta)}\right)^{1/2}-1$. Hence, the total energy to deform the cytoplasm is $U_{cyto}={}^2\!/_3\,\pi R^3 E_{cyto}\left\{\left({}^{\Delta}\!/_{(2R)}\right)^2+2\left(\left({}^{R}\!/_{(R-\Delta)}\right)^{1/2}-1\right)^2\right\}\approx {}^1\!/_2\, E_{cyto}R\Delta^2$.Now consider the elastic energy U_{cortex} to deform the membrane-cortex under a pre-stress tension *T*. By analogy with a string under tension, we have for the spherical cortex:

$$U_{cortex}=\frac{1}{2}T\iint\left(\frac{1}{R}\frac{dw}{d\theta}\right)^2 dA=2\pi T\int_0^{\pi/2}\sin\left(\frac{dw}{d\theta}\right)^2 d\theta\,, \qquad \text{(S15)}$$

where *w* is the radial displacement and θ is a meridian angle. For simplicity, we can approximate ${}^{dw}\!/_{d\theta}\approx {}^{2\Delta}\!/_{\pi}$, hence $U_{cortex}\approx {}^{8T\Delta^2}\!/_{\pi}$. The ratio of energies is ${}^{U_{cyto}}\!/_{U_{cortex}}\approx {}^{\pi^2 E_{cyto}R}\!/_{(16T)}$.

Taking *R*= 8 μm, *T*=700 pN/μm from our AFM data, and E_{cyto}=1-10 Pa (cytoplasm elastic modulus obtained from references; [4, 5]) gives ${}^{U_{cyto}}\!/_{U_{cortex}}$ ≈0.007-0.07. These results taken together make us feel confident that neglecting the elastic response of the cytoplasm is also a good assumption for these cells.

Supporting Information Text S5

The model can fit nonlinear data up to approximately 400 nm Z distance

Additionally, we have made calculations to further show that the model can fit nonlinear data up to approximately 400 nm Z range for force curve obtained on nonadherent HFF cells. The issue raised concerns to the shape of the force-distance curve, which is clearly nonlinear and thus limits the use of the model, which cannot fit the entire curve. The exact force balance equation (Eq. S4) can only fit the data up to 400 nm Z distance as shown in the supporting information figure S6 (Fig. S6). So the model should not be pushed beyond 400 nm, beyond that the model its unreliable. Linearization of the slope is shown by the dotted line, which is all that is required to determine the tension, which makes our method very simple to use.

Supporting Figure S1

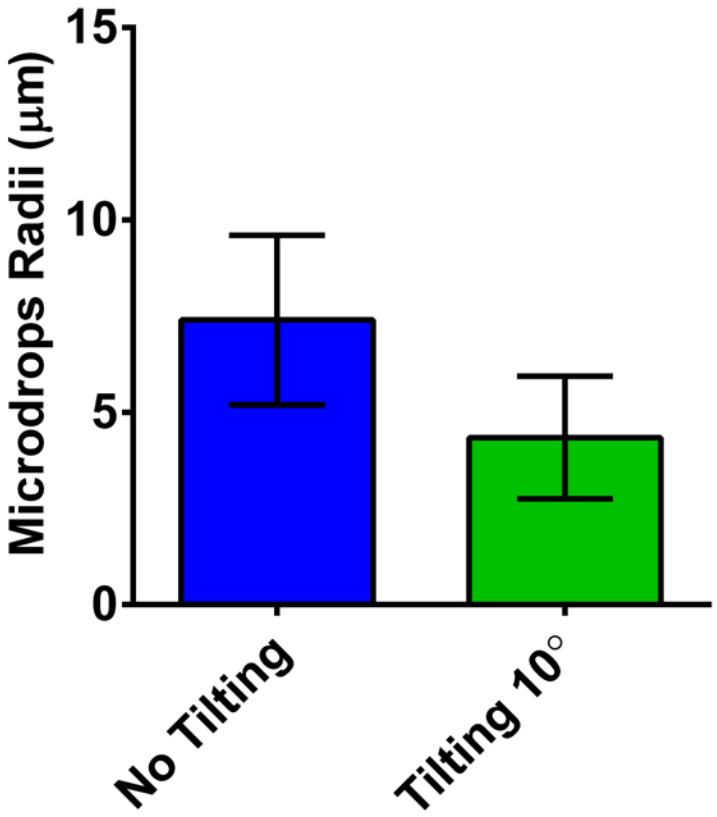

Fig. S1. Water-in-oil microdrops radii distributions for non-tilting and tilting conditions. Measured microdrops radii for the two cases. Cases were found to be statistically significantly different from each other ($p<0.05$). This is because of the inability of generating homogeneous populations by using our microdrops generation method.

Supporting Figure S2

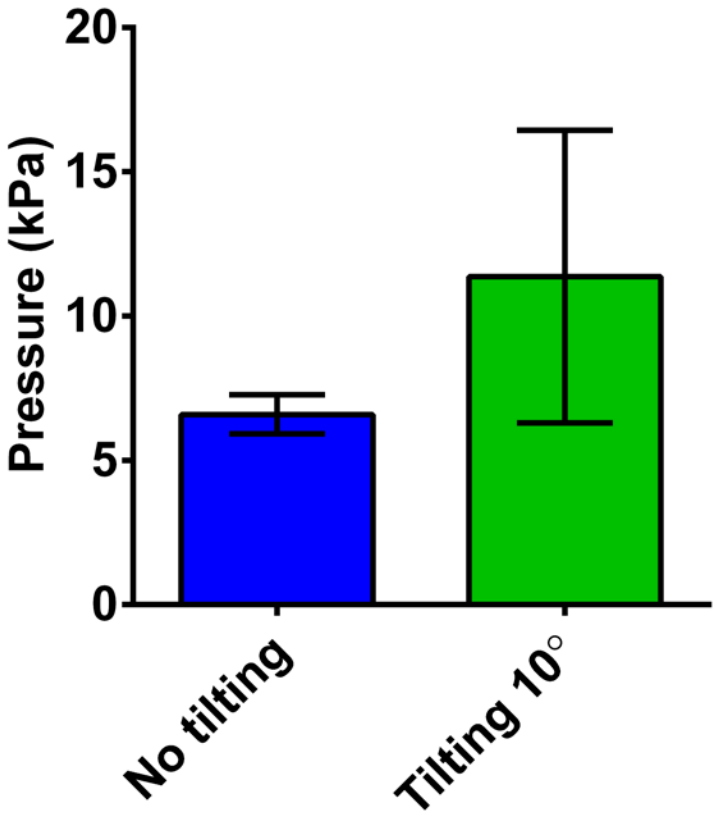

Fig. S2. Calculated hydrostatic pressure of water-in-oil microdrops for non-tilting and tilting conditions. Distribution of calculated hydrostatic pressure for non-tilting and 10° tilting conditions. The differences in measured hydrostatic pressure are due to the inhomogeneity of the generated microdrops radii (Fig. S1).

Supporting Figure S3

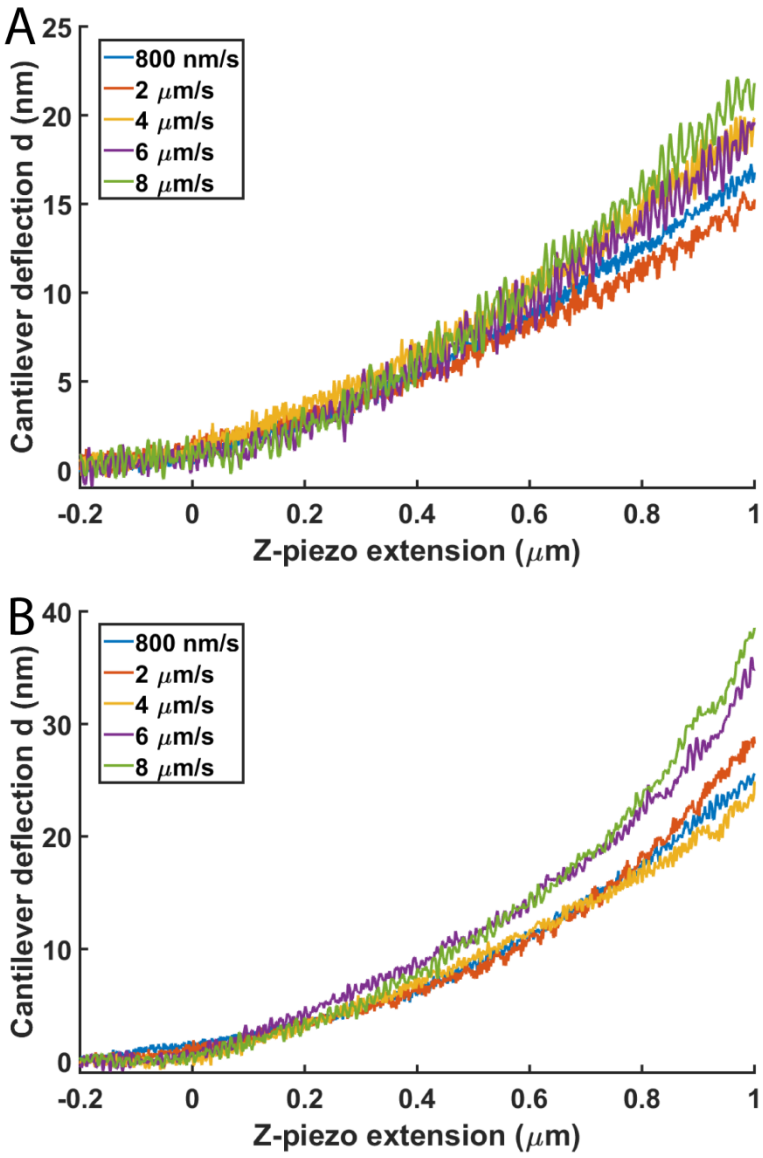

Fig. S3. Velocity-dependent compression force curves performed on the same location for two individual nonadherent HFF cells. (A and B) In both HFF cells successive curves show negligible viscous losses with negligible deviation from each other.

Supporting Figure S4

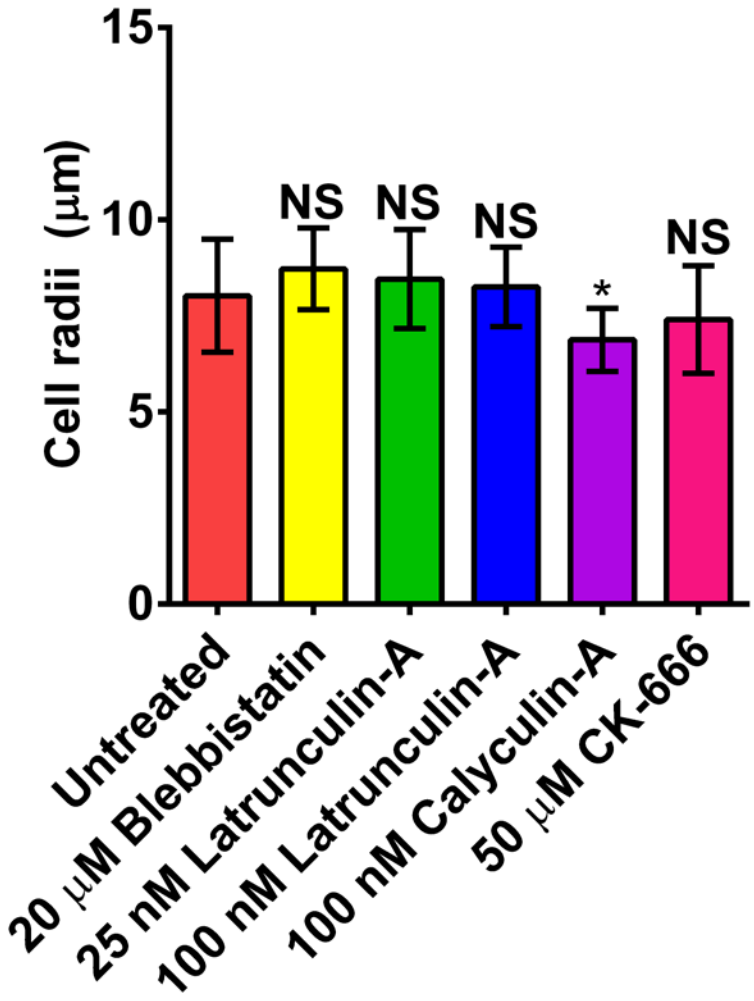

Fig. S4. Cell radii distribution after pharmacological treatments. Measured cell radii of HFF cells after treatments. All cases were found to have not statistical significantly differences ($p>0.05$), except for CA treatment ($p<0.05$).

Supporting Figure S5

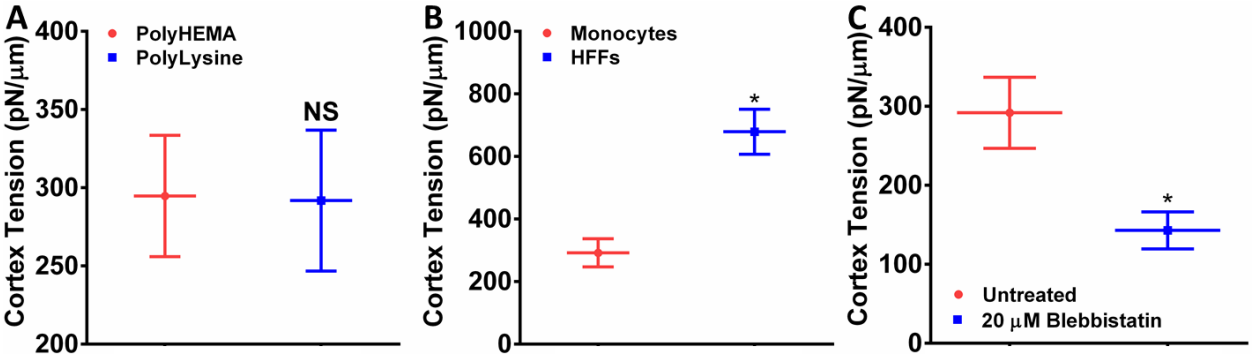

Fig. S5: Determination of nonadherent monocyte cells cortical actomyosin tension. (A) Cortical actomyosin tension for monocytes plated on dishes precoated with low concentrations of polyHEMA and poly-L-lysine. No statistical significant difference was found ($p>0.05$), meaning that low concentrations of poly-L-lysine are safe for measuring the cellular mechanics of passive monocytes. (B) Comparison of extracted cortical tension for HFFs and monocytes. Statistical significant difference was found ($p<0.05$). (C) Monocytes cortical tension after the addition of pharmacological drug 20 μM blebbistatin showing a dramatic decrease compared to untreated cells and with statistical significant difference ($p<0.05$).

Supporting Figure S6

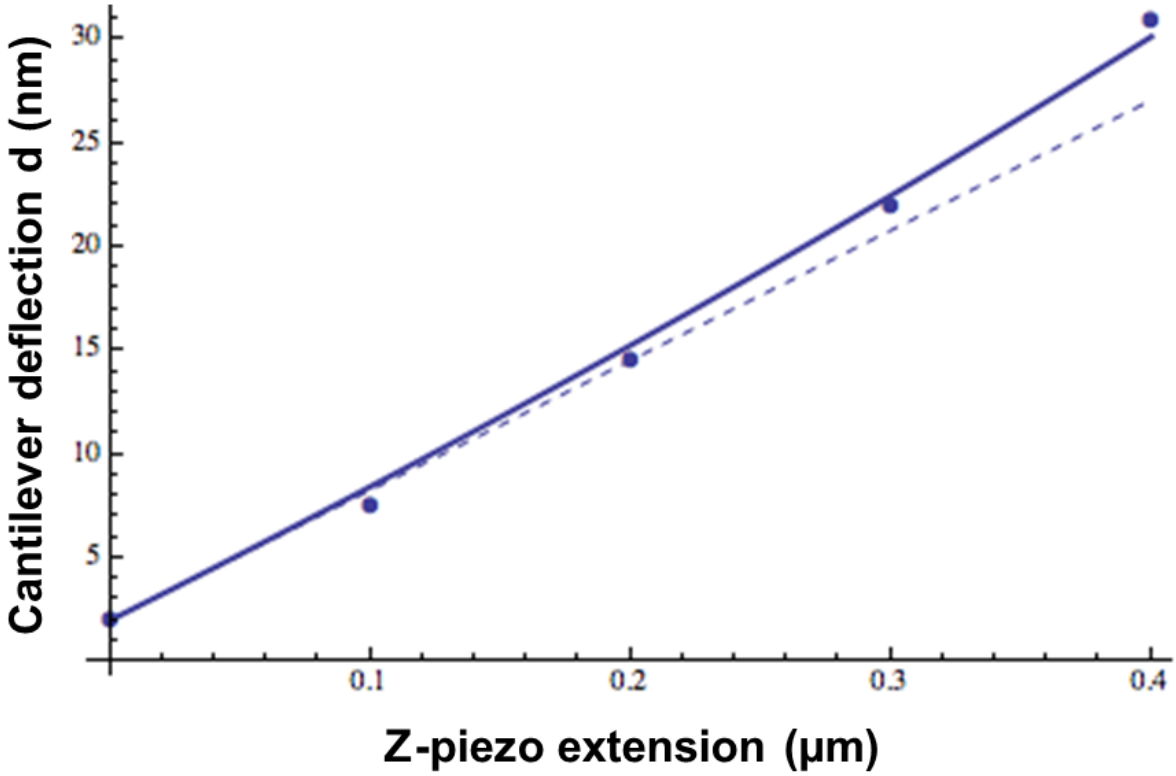

Fig. S6. The model can fit nonlinear data reliable up to 400 nm Z distance range. The data points where taken from Figure 3E and were fit using the supporting equation S4 (Eq. S4) with T= 716 pN/µm and R=6.5 µm. Solid line is the fit using Eq. S4 and dashed line is using Eq. S7 with linearization.

Supporting Figure S7

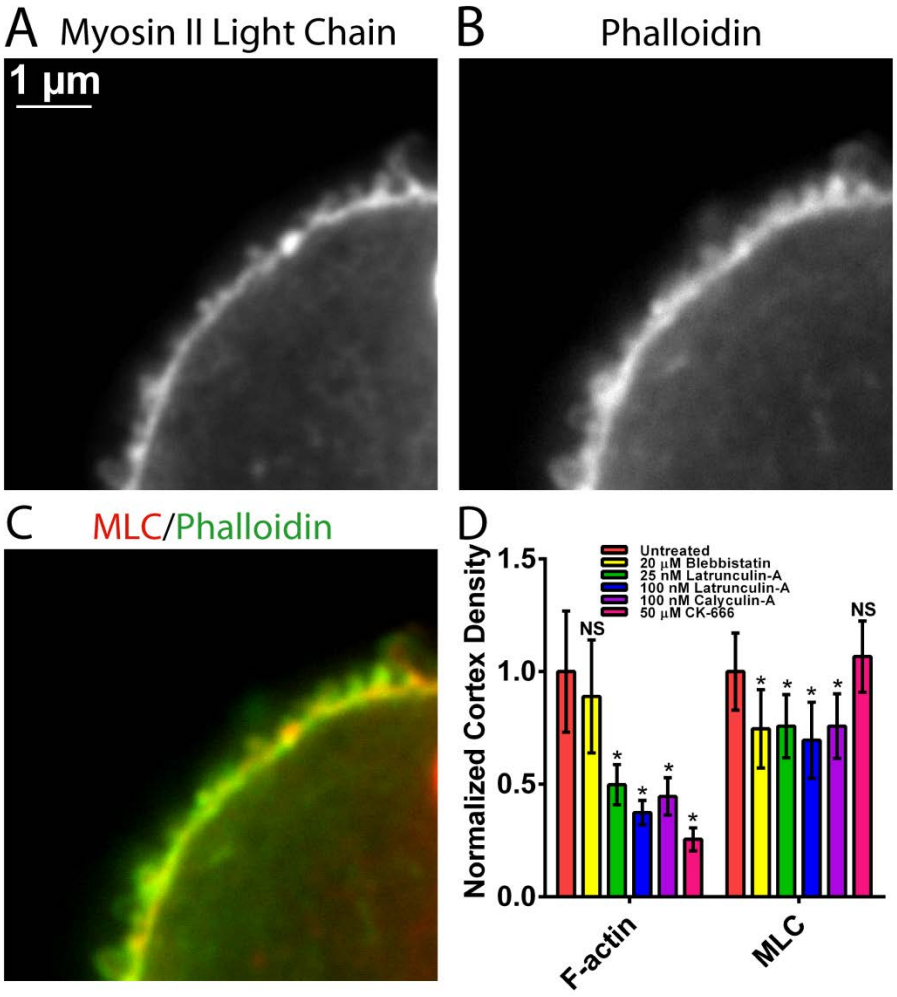

Fig. S7. Myosin II localization in the actin cortex after addition of the pharmacological drugs. (A-C) A representative fixed nonadherent HFF cell labeled for myosin II regulatory light chain with anti-myosin II antibody and for f-actin with Alexa Fluor 564 conjugated-phalloidin were imaged by confocal microscopy. (D) Normalized cortex density of MLC and f-actin measured for untreated and pharmacological treated cells. *$p<0.05$, NS: $p>0.05$.

Supporting Table S1

Table S1. Summary of the bending-to-tensile force ratio.

Parameters	Untreated HFF	20 µM Blebbistatin	25 nM Latrunculin-A	100 nM Latrunculin-A	100 nM Calyculin-A	50 µM CK-666
Cortex tension *T* (pN/µm)	679	379	540	439	1208	1132
Cortex elastic modulus *E* (kPa)	42	22	47	42	67	63
Cell radius *R* (µm)	8	8.7	8.5	8.3	6.9	7.4
Cortex thickness *h* (nm)	146	159	109	93	153	156
Force ratio (Equation S13)	0.0003	0.0003	0.0002	0.0001	0.0005	0.0004

Cortex tension, elastic modulus, thickness, and cell radius are the average value measured and presented in the main text. The bending-to-tensile forces ration was calculated from supporting equation S13 (Eq. S13).

References

1. Gardel, M.L., et al., *Chapter 19 Mechanical Response of Cytoskeletal Networks*, in *Methods in Cell Biology*, J.C. Dr. John and Dr. H. William Detrich, III, Editors. 2008, Academic Press. p. 487-519.
2. Manoussaki, D., et al., *Cytosolic pressure provides a propulsive force comparable to actin polymerization during lamellipod protrusion.* Sci. Rep., 2015. **5**: p. 12314.
3. Zarda, P.R., S. Chien, and R. Skalak, *Elastic deformations of red blood cells.* Journal of Biomechanics, 1977. **10**(4): p. 211-221.
4. Guo, M., et al., *Probing the Stochastic, Motor-Driven Properties of the Cytoplasm Using Force Spectrum Microscopy.* Cell, 2014. **158**(4): p. 822-832.
5. Crick, F.H.C. and A.F.W. Hughes, *The physical properties of cytoplasm: A study by means of the magnetic particle method Part I. Experimental.* Experimental Cell Research, 1950. **1**(1): p. 37-80.